NeuroImage: Clinical 5 (2014) 385–395

Contents lists available at ScienceDirect

NeuroImage: Clinical

journal homepage: www.elsevier.com/locate/ynicl

Regional functional connectivity predicts distinct cognitive impairments in Alzheimer's disease spectrum

Kamalini G. Ranasinghe[a], Leighton B. Hinkley[b], Alexander J. Beagle[a], Danielle Mizuiri[b], Anne F. Dowling[b], Susanne M. Honma[b], Mariel M. Finucane[c], Carole Scherling[a], Bruce L. Miller[a], Srikantan S. Nagarajan[**,b], Keith A. Vossel[*,a,c]

[a]Memory and Aging Center, Department of Neurology, University of California San Francisco, San Francisco, CA 94158, USA
[b]Department of Radiology and Biomedical Imaging, Biomagnetic Imaging Laboratory, University of California San Francisco, San Francisco, CA 94143, USA
[c]Gladstone Institute of Neurological Disease, San Francisco, CA 94158, USA

ARTICLE INFO

Article history:
Received 19 February 2014
Received in revised form 27 June 2014
Accepted 17 July 2014
Available online 23 July 2014

Keywords:
Alzheimer's disease spectrum
Magnetoencephalography (MEG)
Resting-state functional connectivity
Network dysfunction
Posterior cortical atrophy
Logopenic variant PPA

ABSTRACT

Understanding neural network dysfunction in neurodegenerative disease is imperative to effectively develop network-modulating therapies. In Alzheimer's disease (AD), cognitive decline associates with deficits in resting-state functional connectivity of diffuse brain networks. The goal of the current study was to test whether specific cognitive impairments in AD spectrum correlate with reduced functional connectivity of distinct brain regions. We recorded resting-state functional connectivity of alpha-band activity in 27 patients with AD spectrum — 22 patients with probable AD (5 logopenic variant primary progressive aphasia, 7 posterior cortical atrophy, and 10 early-onset amnestic/dysexecutive AD) and 5 patients with mild cognitive impairment due to AD. We used magnetoencephalographic imaging (MEGI) to perform an unbiased search for regions where patterns of functional connectivity correlated with disease severity and cognitive performance. Functional connectivity measured the strength of coherence between a given region and the rest of the brain. Decreased neural connectivity of multiple brain regions including the right posterior perisylvian region and left middle frontal cortex correlated with a higher degree of disease severity. Deficits in executive control and episodic memory correlated with reduced functional connectivity of the left frontal cortex, whereas visuospatial impairments correlated with reduced functional connectivity of the left inferior parietal cortex. Our findings indicate that reductions in region-specific alpha-band resting-state functional connectivity are strongly correlated with, and might contribute to, specific cognitive deficits in AD spectrum. In the future, MEGI functional connectivity could be an important biomarker to map and follow defective networks in the early stages of AD.

1. Introduction

Synchronization of neuronal activity across different brain regions is a fundamental property of cortical networks (Singer, 1999). Spontaneous correlations in activity occur between brain regions that are spatially distributed yet functionally related (Fox and Raichle, 2007). Patterns of temporally coherent fluctuations within widely distributed cortical systems also correspond with behavior (Hampson et al., 2006; Seeley et al., 2007). Large-scale brain networks that are developmentally formed to regulate behavior are also selectively targeted by different neurodegenerative diseases (Seeley et al., 2009).

Alzheimer's disease (AD), the most common age-related dementia, is associated with early disruption of functional neural networks. Structural, molecular, and metabolic changes in the AD brain mirror, to a large extent, the distributed intrinsic network collectively called the default mode network — regions characterized by task-related deactivation on resting-state functional magnetic resonance imaging (fMRI) (Buckner et al., 2005; Seeley et al., 2009). Regions that show the strongest functional connectivity, such as the default mode network, are often the most vulnerable to neurodegenerative disease (Seeley et al., 2009; Zhou et al., 2012). Electroencephalographic (EEG) and magnetoencephalographic (MEG) recordings have demonstrated reductions in global neural synchrony in AD and mild cognitive impairment

Abbreviations: CDR-SOB, Clinical Dementia Rating Sum of Boxes; CVLT, California Verbal Learning Test; fMRI, functional magnetic resonance imaging; lvPPA, logopenic variant primary progressive aphasia; MCI, mild cognitive impairment; MEGI, magnetoencephalographic imaging; MMSE, Mini-Mental State Exam; PCA, posterior cortical atrophy; VOSP, Visual Object and Space Perception.

** Correspondence to: Professor in Residence, Department of Radiology and Biomedical Imaging, UCSF School of Medicine, University of California San Francisco, 513 Parnassus Avenue, S362, San Francisco, CA 94143.

* Correspondence to: Assistant Professor, Gladstone Institute of Neurological Disease, UCSF Memory and Aging Center , 1650 Owens St., San Francisco, CA 94158.

E-mail address: Srikantan.Nagarajan@ucsf.edu (S.S. Nagarajan), KVossel@memory.ucsf.edu (K.A. Vossel).

http://dx.doi.org/10.1016/j.nicl.2014.07.006

(MCI) (de Haan et al., 2008; Jelic et al., 1996; Stam et al., 2009). These changes in synchrony may indicate failing connectivity within large-scale functional networks. The relationship between region-specific network connectivity in AD and domain-specific cognitive dysfunction, however, remains largely unknown.

In this study, we tested the hypothesis that region-specific resting-state functional connectivity patterns are correlated with focal cognitive deficits in AD spectrum. We explored resting-state functional connectivity using MEG imaging (MEGI)-acquired alpha-band oscillations in patients meeting research criteria for probable AD or MCI due to AD. Our results demonstrate the differential involvement of distinct functional networks and the heterogeneous nature of AD. Robust correlations to cognitive deficits indicate region-specific functional connectivity deficits as a potential tool to gauge specific network dysfunctions in AD.

2. Methods

2.1. Subjects

Patients were recruited from research cohorts at the University of California San Francisco (UCSF) Memory and Aging Center, and consisted of 27 patients with AD spectrum, including five with logopenic variant primary progressive aphasia (lvPPA), seven with posterior cortical atrophy (PCA), ten with amnestic/dysexecutive variant, and five with MCI (four amnestic MCI and one language-predominant MCI). All patients underwent a complete clinical history and physical examination, a neuropsychological assessment, and a structured caregiver interview. Diagnosis was made by consensus at a multidisciplinary meeting and was based on clinical evaluation, neuropsychological test performance, and biomarkers (Supplementary Table 1). Of the 23 patients with amyloid imaging and/or CSF analysis for beta-amyloid$_{1\text{–}42}$ peptide and tau protein, 21 had findings supportive of AD. The two subjects that were amyloid imaging negative (one borderline) were both MCI. Each had hippocampal atrophy and deficits in episodic memory, which are strong predictors of conversion to AD (Devanand et al., 2007). Forty-eight percent (11 of 23) of the AD-spectrum cohort with apolipoprotein E (apoE) genotyping were carriers of the apoE4 allele. Patients received the initial diagnosis of probable AD or MCI if they fulfilled the National Institute of Aging–Alzheimer's Association criteria for probable AD or MCI due to AD, respectively (Albert et al., 2011; McKhann et al., 2011). Each probable AD presentation was then reviewed to assess whether patients fulfilled the specific diagnostic criteria for PCA or lvPPA (Gorno-Tempini et al., 2011; Mendez et al., 2002). Patients who met the criteria for probable AD but did not meet criteria for either PCA or lvPPA were categorized into amnestic/dysexecutive variant. We also recruited 15 healthy age-, education-, and sex-matched control subjects (mean age 64.3 ± 5.0, $p = 0.59$, mean education 16.8 ± 2.2, $p = 0.18$, and mean Mini-Mental State Exam score 29.5 ± 0.7, $p < 0.0001$ vs. patients, unpaired t tests; percent male 53%, $p = 0.43$, Chi-square test) for the comparisons of MEG power spectrum analysis and gray matter volume assessment based on structural magnetic resonance imaging (MRI). Informed consent was obtained from all participants or their assigned surrogate decision makers. The study was approved by the UCSF Committee on Human Research.

2.2. Neuropsychological assessment and statistical analysis

Each patient completed the Mini-Mental State Exam (MMSE), Clinical Dementia Rating scale (CDR) and CDR Sum of Boxes (CDR-SOB) (Morris, 1993) (Table 1), and a battery of neuropsychological tests designed to assess executive function, spatial ability, memory, and language function (Table 2). Tasks used to assess the individual domains of cognitive function were detailed in a previous report (Kramer et al., 2003) and included D words, animals, digit span backward, a modified Trail Making Test, Stroop color naming, Stroop interference, Boston Naming Test (BNT), California Verbal Learning Test–Short Form (CVLT) containing 9 items, CVLT 30-second free recall, CVLT 10-minute free recall, Benson copy, Benson free recall, and the number location test of the Visual Object and Space Perception (VOSP) battery. We categorized the fluency tasks under executive function although we acknowledge that they also rely on language (Possin et al., 2014). Given that fewer than 25 patients performed the modified Trail Making Test and Stroop test, we excluded these tasks from the subsequent correlation analyses (Cohen, 1992). We performed one-way-ANOVA with Tukey *post hoc* tests to compare the cognitive scores between subgroups of AD spectrum using SAS (SAS Institute, Cary, NC).

Table 1
Patient demographics.

Age (years)	63.2 ± 7.1
MMSE (/30)	22.5 ± 4.2
Sex (% male)	41
Handedness (% right)	92
Education (years)	15.8 ± 2.2
CDR	0.84 ± 0.3[a]
CDR-SOB	5.1 ± 1.8[a]
Age at onset (years)	57.8 ± 7.1
Disease duration	5.4 ± 3.3

The patient group includes a total of 27 patients with posterior cortical atrophy ($n = 7$), amnestic/dysexecutive ($n = 10$), logopenic variant primary progressive aphasia ($n = 5$), and mild cognitive impairment ($n = 5$). Numbers show means and standard deviations.
CDR = Clinical Dementia Rating, CDR-SOB = Clinical Dementia Rating Sum of Boxes, MMSE = Mini-Mental State Exam.
[a] $n = 26$.

2.3. Magnetic resonance image acquisition

Structural images were acquired on a 3 Tesla Siemens MRI scanner at the Neuroscience Imaging Center-UCSF for 22 of the 27 patients and for all 15 control subjects. The remaining 5 patients were studied using MRI scans obtained at an outside facility within 2 years of their MEG evaluation.

2.4. Magnetoencephalographic image acquisition and processing

MEGI uses MEG sensor data with millisecond precision and applies source reconstruction algorithms to overlay cortical oscillatory activity onto structural brain images. This process enables reconstruction of the oscillatory activity from MEG data in specific brain regions with high spatiotemporal precision.

Each subject underwent MEGI on a 275-channel whole-head MEG system (MISL, Coquitlam, British Columbia, Canada) consisting of 275 axial gradiometers (sampling rate = 600 Hz). Three fiducial coils including the nasion and the left/right pre-auricular points were placed to localize the position of the head relative to the sensor array. These points were later co-registered to a T1-weighted MRI to generate a head shape. Data collection was optimized to minimize within-session head movements to not exceed 0.5 cm. Ten minutes of continuous recording was collected from each subject lying supine, awake, and with eyes closed. We selected a 60-second epoch of contiguous stationary segment of data for MEG source data analysis. The full recording of the data was not used to minimize the inclusion of motion artifact and other potential artifacts. Previous studies have determined that a 60-second window provides reliable, consistent power for reconstruction of brain activity from the resting-state MEG data (Guggisberg et al., 2008; Hinkley et al., 2010; Hinkley et al., 2011). Artifact free segments were selected by using signal amplitudes less than a threshold of 10 pT, and by visually inspecting the sensor data to identify segments without artifacts generated by eyeblinks, saccades, head movements, or muscle contractions. Both controls' and patients' data were within our specified limits of signal scatter, and the two groups had no difference

Table 2
Neuropsychological performance scores.

Neuropsychological test		*n*	PCA	Amn/Dys	lvPPA	MCI	*p*
CDR-SOB		26	5.6 ± 1.6	5.3 ± 1.9	4.6 ± 1.1	4.4 ± 2.4	0.54
Executive function	Lexical fluency	27	**12.1±3.2**	9.2 ± 2.3	**6.2±3.2**	8.8 ± 2.3	< **0.05**
	Category fluency	27	10.0 ± 5.1	11.3 ± 4.2	6.8 ± 3.6	11.2 ± 5.3	0.40
	Modified Trails (lines/s)	22	0.06 ± 0.0	0.2 ± 0.2	0.15 ± 0.1	0.3 ± 0.1	0.21
	Stroop color naming	21	**26±16**	57 ± 25	34 ± 15	**64±14**	< **0.05**
	Stroop inhibition	21	10 ± 8.1	23 ± 15	10 ± 8	32 ± 13	< 0.05
	Digits span backward	27	**2.6±1.3**	3.1 ± 0.7	**2.5±0.6**	**4.4±1.1**	< **0.05**[a]
Language	Boston Naming Test	27	13 ± 5.5	12 ± 3.0	10 ± 3.1	11 ± 1.7	0.68
Visuospatial	Benson copy	27	**3.8±2.1**	**13.1±4.0**	**13.7±1.3**	**15.2±0.8**	< **0.0001**[b]
	VOSP number location	25	**4.1±1.0**	**7.4±2.6**	7.2 ± 3.2	**9.4±0.5**	< **0.01**[c]
Learning & memory	CVLT total score	25	17.2 ± 5.5	17.4 ± 5.8	17 ± 5.3	20 ± 5.3	0.909
	CVLT 30 s recall	25	4.0 ± 2.7	3.4 ± 1.1	5 ± 3.1	4 ± 1.0	0.569
	CVLT 10 m recall	25	2.8 ± 2.7	1.2 ± 1.4	4.2 ± 3.4	2.2 ± 1.7	0.158
	Benson 10 m recall	27	1.8 ± 1.8	1.8 ± 2.9	5.8 ±3.2	5.6 ± 4.6	< 0.05

p values indicate the significance of one-way-ANOVA.
Bold text indicates the groups that were statistically different after Tukey *post hoc* comparison between the patient groups of posterior cortical atrophy (PCA), logopenic variant primary progressive aphasia (lvPPA), amnestic/dysexecutive (Amn/Dys), and MCI, with the significance threshold set to 0.05.
CDR-SOB = Clinical Dementia Rating Sum of Boxes, CVLT = California Verbal Learning Test, VOSP number location = number location task of Visual Object and Space Perception battery, 30 s = 30 seconds, 10 m = 10 minutes. Shown are means and standard deviations.
[a] MCI vs. lvPPA and PCA
[b] PCA vs. MCI, lvPPA, and Amn/Dys groups.
[c] PCA vs. MCI and Amn/Dys groups.

in head movement (unpaired *t* test comparing the degree of head movement before and after the resting data segment. Mean ± SD for patients = 0.34 ± 0.28 cm, controls = 0.27 ± 0.18 cm; t = 0.85, $p = 0.4$).

In the current study we used a 20-mm isotropic grid in the sensor space, and reconstructed into source space using a minimum-variance adaptive spatial filtering technique (Dalal et al., 2008). Tomographic reconstructions of the MEG data were generated using a head model based on each subject's structural MRI. Each subject's T1-weighted MRI was spatially normalized to the standard Montreal Neurological Institute template brain using standardized procedures (5 mm voxels; SPM2 http://www.fil.ion.ucl.ac.uk/spm/software/spm2) (Ashburner and Friston, 1999). The results of normalization were manually verified in all subjects. A whole brain volume of interest for lead field computation was generated by transformation of all the points within a spatially normalized MRI that corresponded to locations within the brain and excluded non-cerebral points. Source-space MEGI analysis and functional connectivity were generated using the NUTMEG software suite (http://nutmeg.berkeley.edu) (Dalal et al., 2011). For source-space reconstructions, the MEG sensor data were filtered with a phase-preserving bandpass filter (fourth-order Butterworth; 1–20 Hz). The source-space reconstruction approach allowed amplitude estimates at each voxel derived through a linear combination of a spatial weighting matrix with the sensor data matrix (Hinkley et al., 2011). The alpha frequency peak, identified as the greatest power density within the 8–12 Hz range for each subject was chosen to select a subject-specific alpha band. Mean alpha power of a 4-Hz window around this peak was used for the subsequent functional connectivity analysis. Previous studies have shown that, out of a range of frequency bands, the alpha-band connectivity maps provide the greatest within-session and cross-session reliability measurements and highest signal-to-noise ratio (Guggisberg et al., 2008; Hanslmayr et al., 2011; Hindriks et al., 2011; Hinkley et al., 2012; Hinkley et al., 2011; Klimesch, 1999; Palva et al., 2010; Westlake et al., 2012).

We computed imaginary coherence, which is a reliable metric for functional connectivity with MEG reconstruction (Engel et al., 2013; Guggisberg et al., 2008; Martino et al., 2011; Nolte et al., 2004). Coherence-measures quantify the strength of neural oscillations. An important limitation of coherence is the introduction of signal mixing artifacts, where a single active source contributes to the other sensors through volume spread. We chose imaginary coherence because it captures only the coherence that cannot be explained by volume spread, and thus gives more accurate results. Previous studies have demonstrated that imaginary coherence reduces overestimation biases of MEG data and is able to sample interactions between source time-series, independent of the class of spatial filter used (Guggisberg et al., 2008; Martino et al., 2011; Nolte et al., 2004). In addition, more recent studies utilizing MEG in preoperative assessments have demonstrated the biological significance of imaginary coherence in evaluating functional connectivity (Martino et al., 2011; Tarapore et al., 2012). A single voxel's Fisher's Z-transformed imaginary coherence values between that voxel and all other voxels in the grid were averaged to compute the global connectivity at each voxel. Global connectivity, represented by the mean imaginary coherence measure in our study, would be akin to mean path-length of the maps of graph theoretic measures.

Neuropsychological measures from each patient, including the CDR-SOB and cognitive test scores, were correlated with global connectivity values at each voxel using the Pearson's correlation. For all voxel-wise functional connectivity correlations with neuropsychological scores that survived an uncorrected $p < 0.05$, we performed a multiple comparisons correction using a False Discovery Rate (FDR) set at 10% (Benjamini and Hochberg, 1995). When effects were significant, we explored how robust these effects were by applying a more stringent threshold, with an FDR cutoff value of 5%. We report the most conservative multiple comparisons correction producing significant effects. Control subjects were excluded from this analysis because their high scores and low variability on the neuropsychological measures created ceiling effects that precluded such correlations. Group comparison of spectral power between the patient group and the control group was done by using an unpaired *t*-test.

2.5. Voxel based morphometry

The voxel based morphometry (VBM) analysis used subjects with 3 Tesla MRI scans ($n = 22$ patients and 15 controls) to maintain consistency across subjects and to generate quality data for atrophy pattern assessments. We assessed the gray matter volume variations of patients and controls using standard methods of optimized VBM procedures within the VBM8 toolbox of statistical parametric mapping version 8 (SPM8) (http://www.fil.ion.ucl.ac.uk/spm/software/spm8/). SPM8 is equipped with an Expectation Maximization Segmentation tool for tissue segmentation to obtain probabilistic maps of gray matter and white matter. After tissue segmentation, gray matter probabilistic maps

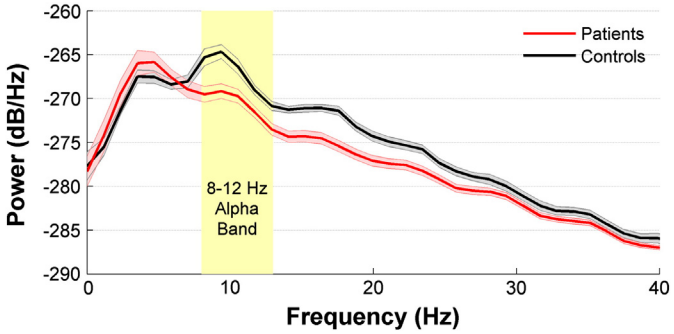

Fig. 1. Averaged power spectral density estimates for different frequency bands. AD-spectrum patients showed decreased power of higher frequency activity over the alpha ($p < 0.01$), beta ($p < 0.01$) and gamma range ($p = 0.08$), and an apparent increase of power in lower frequency activity over the delta and theta range (nonsignificant), compared to age-matched healthy controls. Alpha range is highlighted in yellow. Shaded zone around each line depicts standard error. Spectral data were derived from MEG sensors. $n = 27$ patients, $n = 15$ controls.

of all subjects were initially transformed into the standard Montreal Neurological Institute space. The segmented gray matter probabilistic maps in their respective native space were then spatially normalized again to the population-based templates using a nonlinear transformation. Jacobian modulation was performed to obtain the volume differences from the spatially normalized gray matter image. The modulated images were smoothed with a 12-mm full-width-at-half-maximum isotropic Gaussian kernel to be used for group analyses.

Group comparisons between patient subgroups and the control group were done using unpaired *t*-tests. Significant group differences were identified at family-wise error $p < 0.05$ unless otherwise indicated. Age was included as a nuisance covariate. We also performed an analysis in which we correlated each of the voxel-wise volume estimates with the neuropsychological performance scores, while keeping the total intracranial volume and age as covariates. Significant clusters of correlation were determined using height and extent thresholds of $p < 0.001$ uncorrected, at cluster level.

2.6. Bayesian validation analysis

A Bayesian hierarchical model was used to further validate the results from the correlation analysis. This analysis considered the significantly correlated voxels within an immediate cluster around the peak voxel (i.e., voxel that shows the strongest correlation). To maintain consistency of voxel-cluster selection across different cognitive tasks, we kept it limited to the immediate cluster of 27 connected voxels in three-dimensional space. For comparability across tests, we standardized the scores from each test (by subtracting off the mean score and dividing by the standard deviation). Let y_{ivt} denote the standardized score of subject i corresponding to voxel v on test t. The likelihood of our model was given by:

$$y_{ivt} = \beta_{vt} x_{iv} + b_i + \varepsilon_{ivt},$$

where β_{vt} is the effect on the score of test t of the connectivity (imaginary coherence) (x_{iv}) of voxel v. The random effect b_i captures the correlation of repeated measurements on subject i. The error term ε_{ivt}

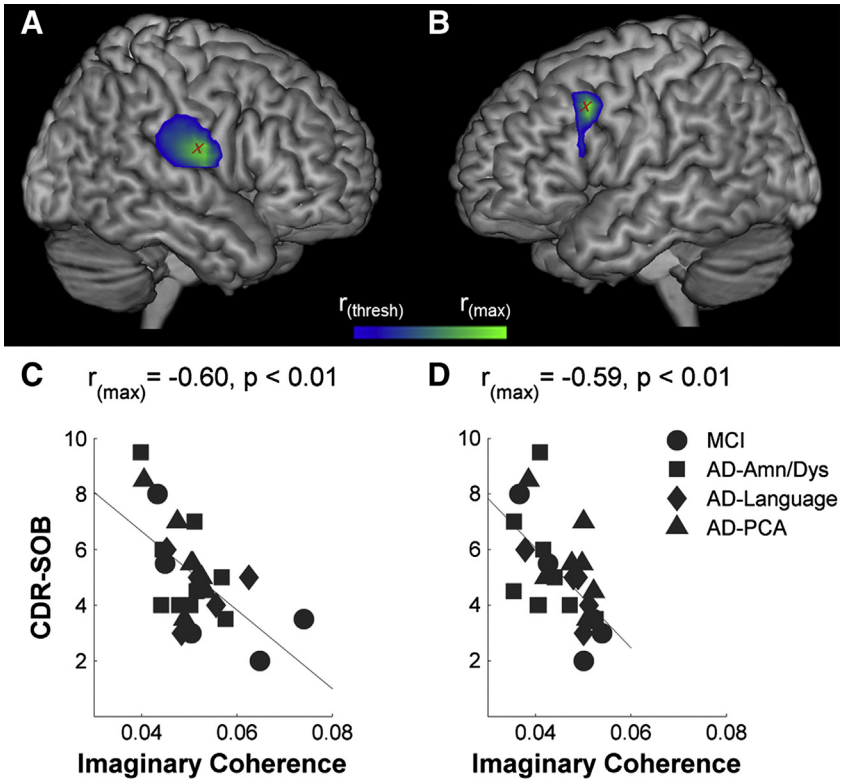

Fig. 2. Reduced resting-state functional connectivity is correlated with disease severity in multiple brain regions in AD spectrum. Imaginary coherence, reflecting the resting-state alpha-band global functional connectivity, predicts the degree of disease severity, as measured by the clinical dementia rating sum of boxes (CDR-SOB). The voxel containing the peak correlation between CDR-SOB and imaginary coherence identified over the right posterior perisylvian region (indicated by the "X" in panel (A) and plotted in panel (C)), and over the left frontal cortex (indicated by the "X" in panel (B) and plotted in panel (D)) are shown. Voxel-wise multiple comparisons are thresholded with 5% FDR correction. Statistical maps are superimposed on a rendering of the Montreal Neurological Institute template brain. The color scheme is normalized to the peak voxel correlation. *p* values on scatter plots indicate corrected *p* value for the peak voxel correlation. $n = 27$ patients. MCI = mild cognitive impairment, AD = Alzheimer's disease, PCA = posterior cortical atrophy, Amn/Dys = amnestic/dysexecutive, AD-Language = logopenic variant primary progressive aphasia, CDR-SOB = Clinical Dementia Rating Sum of Boxes, $r_{(thresh)}$ = correlation coefficient at the 5% FDR threshold, $r_{(max)}$ = correlation coefficient of the peak voxel.

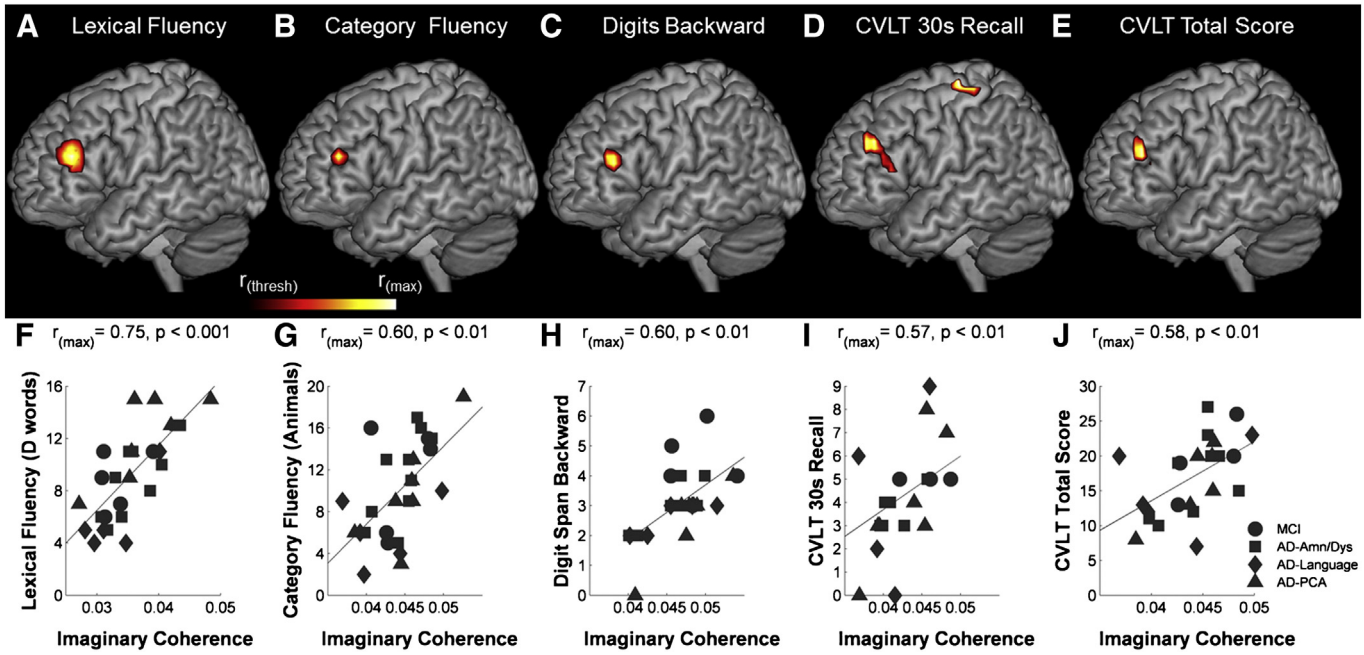

Fig. 3. Resting-state functional connectivity deficits in the left dorsolateral prefrontal cortex correlate with impairments in cognitive performance in AD spectrum. Resting-state functional connectivity as measured by imaginary coherence of the left dorsolateral prefrontal cortex correlated with performance of (A, F) lexical fluency (D words), (B, G) category fluency (animals), (C, H) digit span backward, (D, I) CVLT 30-second recall, and (E, J) CVLT total score. Performance on CVLT 30-second recall also correlated with functional connectivity of the left postcentral gyrus. Statistical maps were corrected at cluster level (20 voxels) across the whole brain. The scatter plots show the peak voxel correlations. Voxel-wise multiple comparisons are thresholded with 5% FDR correction. Statistical maps are superimposed on a rendering of the Montreal Neurological Institute template brain. The color scheme of each image is normalized to the peak voxel correlation with the respective neuropsychological score. *p* values on scatter plots indicate corrected *p* value for the peak voxel correlation. The corresponding *r* values and corrected *p* values at the 5% FDR threshold ($r_{(thresh)}$) include: lexical fluency, $r = 0.4825$, $p = 0.0093$; category fluency, $r = 0.4785$, $p = 0.01$; digit span backward, $r = 0.4795$, $p = 0.0098$; CVLT 30 s recall, $r = 0.499$, $p = 0.0095$; CVLT total score, $r = 0.497$, $p = 0.0098$. MCI = mild cognitive impairment, AD = Alzheimer's disease, PCA = posterior cortical atrophy, Amn/Dys = amnestic/dysexecutive, AD-Language = logopenic variant primary progressive aphasia, CVLT = California verbal learning test, $r_{(thresh)}$ = correlation coefficient at the 5% FDR threshold, $r_{(max)}$ = correlation coefficient of the peak voxel.

describes residual variability due to measurement error and other unmeasured factors. We specified a hierarchical prior for β_v:

$$\beta_v \sim N(\beta_t, \sigma^2{}_v)$$

$$\beta_t \sim N(\beta_f, \sigma^2{}_t)$$

$$\beta_f \sim N(\beta, \sigma^2{}_f)$$

The voxel-specific effects (β_v) are centered around their test-level counterparts (β_t), which are in turn centered around the domain-level effects (β_f), which are in turn all centered around a common global β. Domain-level effects correspond to the tests grouped as executive, visuospatial, and episodic memory categories, each reflecting a specific cognitive domain. The error terms are modeled as normal with mean zero and variance $\sigma^2{}_\varepsilon$. The global β and all four σs are given non-informative flat priors. The b_i are modeled as $N(0, \tau^2)$.

We fit the model with the Markov chain Monte Carlo (MCMC) algorithm using the statistical programming language R (http://www.R-project.org) to estimate the posterior distribution of each parameter. The 95% credible intervals represent the 2.5–97.5 percentiles of the posterior distribution. Additional multiple comparisons corrections are not required in the Bayesian hierarchical model since the shrinkage prior, which shifts estimates towards each other, results in 'partial pooling', a compromise between the overly simplistic global-level estimate and the overly noisy voxel-specific estimate. This method is well described in the statistical literature (Gelman et al., 2012). We started three MCMC chains from over-dispersed initial values. After 5000 iterations of burn-in, we obtained 5000 additional samples from each chain. Convergence was achieved, with all chains having Gelman Rubin statistics of 1 (Gelman and Rubin, 1992). We combined the three chains and thinned to obtain 5000 iterations with which to do inference. Mixing sufficed to yield > 2500 effectively independent samples (Plummer et al., 2006) from each chain.

3. Results

3.1. AD-spectrum patients have reduced resting-state alpha activity and reduced functional connectivity that correlates with higher disease severity

Consistent with previous reports (de Haan et al., 2008; Jeong, 2004), in a quantitative power analysis of MEG data, AD-spectrum patients showed significant slowing of alpha-band (8–12 Hz) activity compared to an age-matched control group (Fig. 1). To measure functional connectivity, we computed imaginary coherence within the alpha band at each voxel (see Methods for details) depicting the connectivity of a given voxel to the rest of the brain. We found that functional connectivity is inversely related to CDR-SOB (degree of disease severity) in AD spectrum. Higher CDR-SOB correlated with reduced levels of imaginary coherence in clusters localized in the right posterior perisylvian region and left middle frontal cortex. The strongest correlation was seen over the right posterior perisylvian region (Fig. 2A and C) and the second strongest was over the left frontal cortex (Fig. 2B and D). These results indicate that neuronal synchronization of spatially distributed regions of the brain is significantly correlated with the global cognitive disability in AD spectrum.

3.2. Subgroups within AD spectrum have distinct patterns of cognitive dysfunction

Neuropsychological measures of specific cognitive domains have reliably distinguished between distinct clinical variants of AD spectrum (Rabinovici et al., 2010). Consistent with these earlier reports, patients in the lvPPA, PCA and amnestic/dysexecutive subgroups in our study showed unique profiles of cognitive performance (Table 2). For example, PCA patients had better lexical fluency scores (e.g., D word generation) than lvPPA patients ($p < 0.05$, one-way-ANOVA, Tukey *post hoc*), yet performed poorer in visual construction (e.g., Benson copy) than all other subgroups ($p < 0.0001$, one-way-ANOVA Tukey *post hoc*). Other measures that differed significantly among the clinical subgroups included digit span backward (worse in PCA and lvPPA than MCI), VOSP number location (worse in PCA than amnestic/dysexecutive variant and MCI), and Stroop color naming (worse in PCA than MCI). We predicted that resting-state functional connectivity deficits could account for impairments of specific cognitive functions in AD spectrum. Specifically we tested the hypothesis that poor cognitive performance would be correlated with low imaginary coherence measures of brain areas that are important for each task.

3.3. Regional patterns of resting-state functional connectivity are correlated with focal cognitive impairments in AD spectrum

With regards to executive function, we found that lexical fluency, category fluency, digit span backward, short-delay verbal memory, and verbal learning were each significantly correlated with the functional connectivity of the left dorsolateral prefrontal cortex (Fig. 3A–E, Supplementary Table 2). Lower resting-state functional connectivity of this region predicted worse executive performance. lvPPA patients generally scored low in lexical fluency and had low functional connectivity in the left dorsolateral prefrontal cortex, whereas PCA patients generally scored high on lexical fluency and had high functional connectivity in this region (Fig. 3A and, 3F triangles vs. diamonds). Interestingly, one subject met criteria for PCA yet had lower scores in lexical fluency than is typical for PCA; this individual showed relatively poor connectivity of the left dorsolateral prefrontal cortex compared to other PCA subjects who performed better in lexical fluency (3F). This case illustrates associations between phenotypes and network connectivity that would not be predicted from clinical sub-classification alone.

We next searched for brain regions where visuospatial function would correlate with MEGI functional connectivity in AD spectrum. Visual construction ability (Benson copy) and location discrimination ability (VOSP number location) correlated with the degree of resting-state connectivity of the left inferior parietal cortex (Fig. 4, Supplementary Table 2). Weak resting-state functional connectivity of the left inferior parietal cortex predicted poor visuospatial ability. PCA patients had low scores in Benson copy compared to lvPPA patients and likewise showed low functional connectivity over the left inferior parietal cortex in relation to lvPPA patients (Fig. 4C).

Finally, we searched for brain regions where episodic memory function would correlate with MEGI functional connectivity. Delayed verbal memory (CVLT 10-minute recall) defects correlated with connectivity

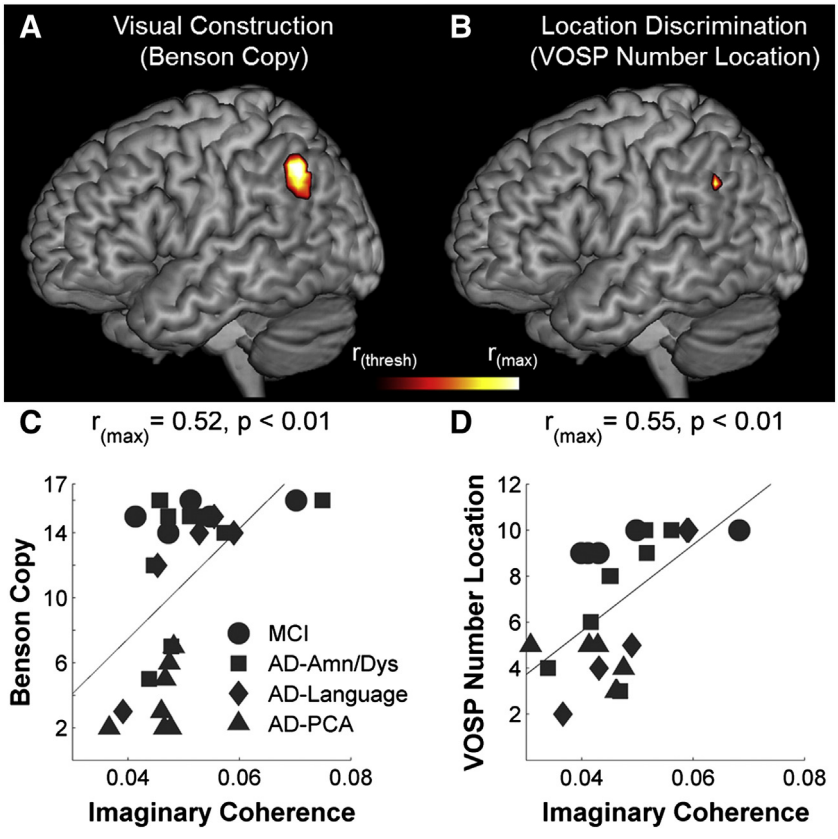

Fig. 4. Resting-state functional connectivity deficits in the left inferior parietal cortex correlate with impairments in visuospatial ability in AD spectrum. Resting-state functional connectivity of the left inferior parietal cortex correlated with performance on the spatial tasks of (A, C) visual construction (Benson copy), and (B, D) location discrimination (visual object and space perception (VOSP) number location). The scatter plots show the peak voxel correlations. Voxel-wise multiple comparisons are thresholded with 10% FDR correction. Statistical maps are superimposed on a rendering of the Montreal Neurological Institute template brain. The color scheme of each image is normalized to the peak voxel correlation with the respective neuropsychological score. *p* values on scatter plots indicate corrected *p* value for the peak voxel correlation. The corresponding *r* values and corrected *p* values at the 10% FDR threshold ($r_{(thresh)}$): visual construction, $r = 0.48$, $p = 0.0097$; location discrimination, $r = 0.5155$, $p = 0.0099$. MCI = mild cognitive impairment, AD = Alzheimer's disease, PCA = posterior cortical atrophy, Amn/Dys = amnestic/dysexecutive, AD-Language = logopenic variant primary progressive aphasia, VOSP number location = number location task of Visual Object and Space Perception battery, $r_{(thresh)}$ = correlation coefficient at the 10% FDR threshold, $r_{(max)}$ = correlation coefficient of the peak voxel.

deficits in the left medial frontal association regions, whereas Benson recall defects correlated with connectivity deficits in the left lateral frontal association regions (Fig. 5A and C, Supplementary Table 2). The amnestic/dysexecutive subgroup showed the lowest scores in episodic memory and also the weakest functional connectivity of the left frontal association regions (Fig. 5B and D).

Collectively, these results support our hypothesis that region-specific functional connectivity deficits are associated with specific cognitive defects in AD spectrum. Whole-brain analysis revealed no regions in which higher functional connectivity associated with worse performance on any of the neuropsychological tests assessed above. Additionally, we found no regions where functional connectivity correlated with language performance on the BNT. Given that AD-spectrum patients generally performed well on this task (Table 2), we were likely underpowered to detect the degree of effect size that was observed in the other cognitive domains.

We performed a Bayesian validation analysis to 1) account for multiple testing and 2) ensure that the cluster of voxels around the peak voxel — and not just the voxel with the strongest correlation — contained a significant association with the neuropsychological score (see methods for details). The validation analysis quantified the effect of connectivity (imaginary coherence) of the voxels in each cluster on each of the cognitive test scores or CDR-SOB, and estimated the difference in each measure per unit change in imaginary coherence (Fig. 6). For example, the standard deviation of scores on the lexical fluency was 3.41. Therefore, the estimated effect of 0.25 indicates that, across voxels in that region, a 0.01 unit increase in imaginary coherence is associated with a $3.41 \times 0.25 = 0.85$ unit increase in the lexical fluency score. None of the confidence intervals (indicated by thin bars for each cognitive task) crossed zero, indicating that all estimated effects are statistically significant. This analysis revealed that after accounting for multiple comparisons and for the cluster of voxels in each region (as opposed to the peak voxel), there was still a significant relationship between functional connectivity and cognitive measures. The Bayesian analysis, depicted in Fig. 6, represents a unifying "meta-analysis" of our data across both spatial and cognitive domains.

3.4. Regional atrophy patterns did not account for correlations between functional connectivity deficits and specific cognitive impairments in AD spectrum

Neurodegenerative diseases cause loss of neurons and neuropil, which is accompanied by gray matter atrophy. The extent to which early cognitive and functional connectivity deficits directly relate to atrophy is unclear. Using a voxel based morphometric assessment we examined the gray matter atrophy patterns of AD. Consistent with previous reports the PCA patients showed atrophy predominantly in temporo-parietal-occipital regions (Fig. 7A), while the lvPPA patients showed atrophy predominantly over the left temporo-parietal cortex (Fig. 7C). The amnestic/dysexecutive subgroup showed mild-

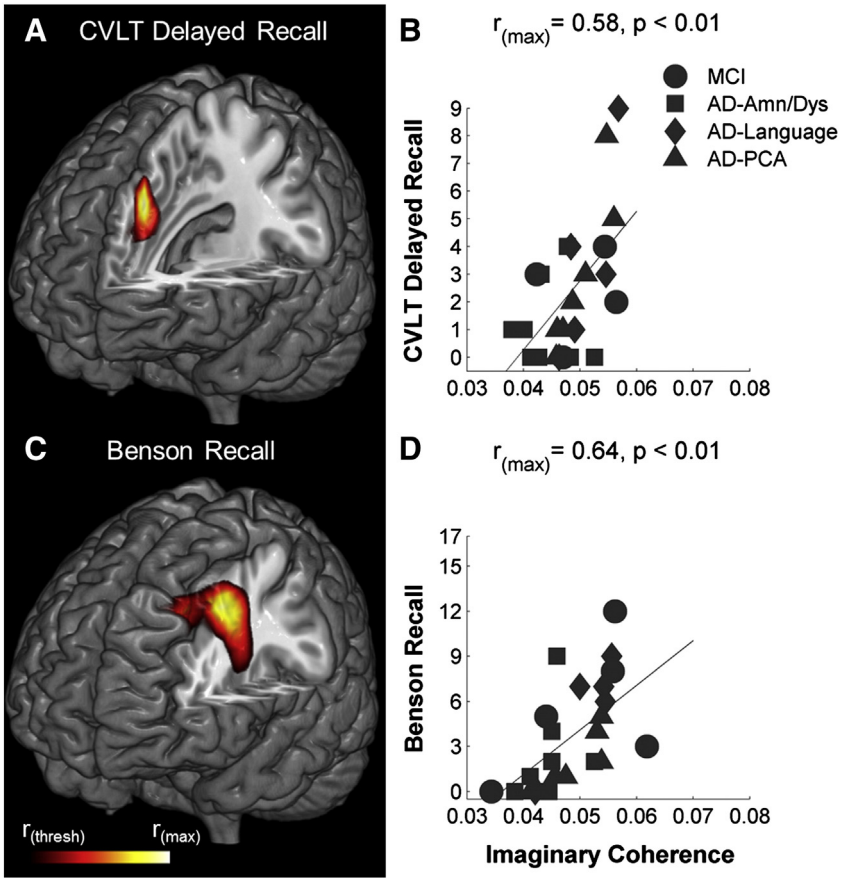

Fig. 5. Resting-state functional connectivity deficits in frontal association regions correlate with impairments in episodic memory performance in AD spectrum. Resting-state functional connectivity of two distinct frontal association regions correlated with performance on the episodic memory tasks (A, B) CVLT delayed recall (verbal memory) and (C, D) Benson recall (visual memory). CVLT delayed recall was related to a relatively medial region of the left frontal cortex (A), whereas Benson recall was related to a relatively more posterior and lateral region in the left frontal cortex (C). The scatter plots show the peak voxel correlations. Voxel-wise multiple comparisons are thresholded with 5% FDR correction. Statistical maps are superimposed on a rendering of the Montreal Neurological Institute template brain. The color scheme of each image is normalized to the peak voxel correlation with the respective neuropsychological score. *p* values on scatter plots indicate corrected *p* value for the peak voxel correlation. The corresponding *r* values and corrected *p* values at the 5% FDR threshold ($r_{(thresh)}$): CVLT delayed recall, $r = 0.498$, $p = 0.0096$; Benson recall, $r = 0.4795$, $p = 0.0098$. MCI = mild cognitive impairment, AD = Alzheimer's disease, PCA = posterior cortical atrophy, Amn/Dys = amnestic/dysexecutive, AD-Language = logopenic variant primary progressive aphasia, CVLT = California verbal learning test, $r_{(thresh)}$ = correlation coefficient at the 5% FDR threshold, $r_{(max)}$ = correlation coefficient of the peak voxel.

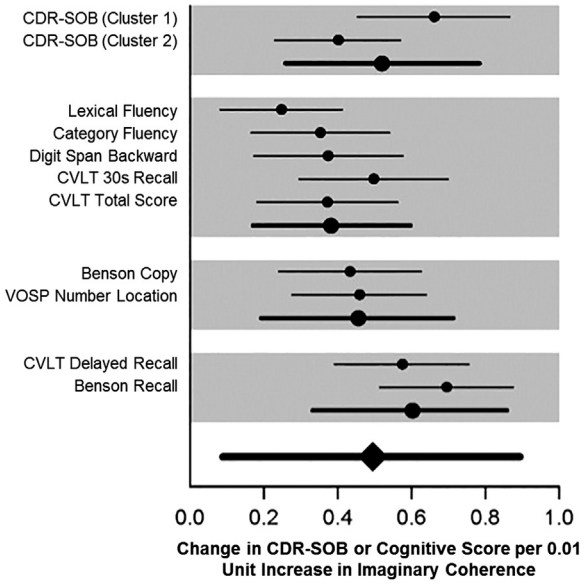

Fig. 6. Bayesian hierarchical validation analysis. The thin horizontal lines show 95% confidence intervals for the estimated associations (βs), which quantify the effect of functional connectivity (imaginary coherence) of the voxels in each cluster on each of the test scores. The four medium-width lines show βs for clinical dementia rating sum of boxes (CDR-SOB) and each of the main cognitive domains (from top to bottom: executive function, visuospatial ability, and memory). The thick line at the bottom of the figure shows the global-level β. For comparability across measures, each score was standardized by subtracting off the mean score and dividing by the standard deviation. CVLT = California verbal learning test, VOSP number location = number location task of the Visual Object and Space Perception battery.

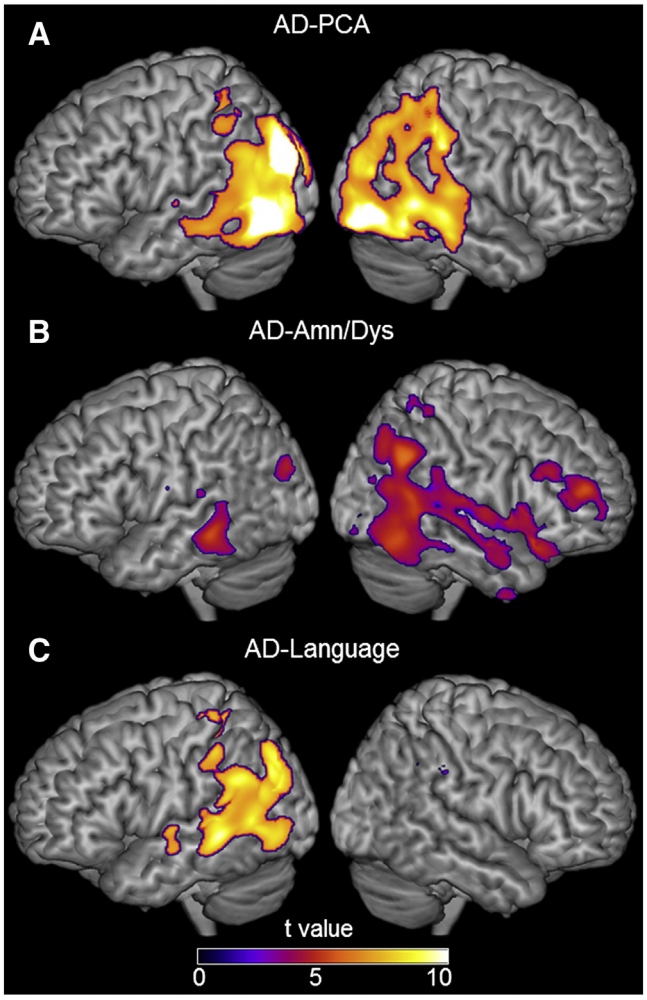

Fig. 7. Voxel based morphometry (VBM)-derived atrophy patterns for different clinical variants of AD. VBM atrophy maps based on comparisons with age-matched healthy controls are shown for the three clinical variants of Alzheimer's disease: (A) posterior cortical atrophy (PCA), (B) amnestic/dysexecutive subgroup (Amn/Dys), and (C) logopenic variant primary progressive aphasia (AD-Language). Regions of gray matter atrophy are shown on the 3-dimensional rendering of the Montreal Neurological Institute (MNI) standard template brain. Results for PCA and AD-Language were corrected for family-wise error ($p < 0.05$) and the results for the amnestic/dysexecutive subgroup were thesholded for uncorrected $p < 0.001$. MNI coordinates and corresponding t values are provided in Supplementary Table 3. $n = 7$ PCA, $n = 7$ amnestic/dysexecutive, and $n = 4$ AD-Language.

to-moderate atrophy in the left hippocampus and bilaterally in the temporo-occipital and frontal cortices (Fig. 7B). The MCI subgroup ($n = 4$) was not significantly different from controls.

We searched for brain regions where gray matter atrophy would correlate with deficits in CDR-SOB or cognitive performance using an approach that was comparable to our functional connectivity analysis. We used the same tasks that were found to have significant correlations between cognitive impairments and functional connectivity defects. These included lexical fluency, category fluency, digit span backward, Benson copy, and VOSP number location. We failed to identify any clusters that showed significant correlations between CDR-SOB or specific cognitive deficits and focal atrophy patterns (Supplementary Table 4). To more carefully scrutinize regions that were identified in our functional connectivity analysis, we pre-selected cortical regions that were localized in the MEGI analysis and searched for correlations between the gray matter volume estimates of these regions and CDR-SOB or related cognitive function (Supplementary Fig. 1). This analysis also revealed no significant correlations between the volume estimates and the neuropsychological measures. Thus, in our cohort, the volume estimates obtained by MRI appeared to be less sensitive predictors of cognitive dysfunction than abnormal neural synchronization patterns detected by MEGI.

4. Discussion

In this study, we showed direct correlations between specific cognitive impairments and deficits in regional functional network connectivity in AD spectrum. Several unique features of our investigation enabled these novel observations: 1) our methodology was unbiased and did not preselect neural networks to interrogate, 2) we performed the MEG analysis in source space (brain space) rather than sensor space enabling us to examine brain-region specific connectivity patterns, 3) we directly measured electrodynamic changes in alpha activity rather than low-frequency hemodynamic changes that are measured with fMRI, and 4) our study population comprised three clinical subtypes of AD as well as MCI, which enhanced the sample heterogeneity and increased the likelihood of identifying distinct patterns of network dysfunction. The degree of gray matter atrophy in our cohort did not correlate with cognitive dysfunction. Although a direct comparison of the MEGI-derived functional connectivity index and the MRI-derived gray matter volume index is beyond the scope of this paper, stronger correlations between MEGI and cognitive performance suggest that abnormalities in resting-state functional connectivity are more sensitive indicators of early cognitive dysfunction than atrophy patterns. Our results demonstrate that region-specific neural dysconnectivity patterns are a potentially useful and precise tool to map and follow defective networks in the early stages of AD.

These findings complement and extend upon previous electrophysiological studies of AD. Tools that allow mapping of distributed functional networks such as EEG and MEG have demonstrated distinct patterns of abnormal connectivity in AD spectrum (Brenner et al., 1986; de Haan

et al., 2008; de Haan et al., 2012b; Duffy et al., 1984; Martin-Loeches et al., 1991). Previous reports revealed predominantly left hemispheric decreased global alpha and beta-band connectivity and increased parietal theta connectivity in AD (de Haan et al., 2012a; de Haan et al., 2008; de Haan et al., 2012b; Osipova et al., 2005; Stam et al., 2009; Stam et al., 2006). The current results demonstrate that focal patterns of alpha dysconnectivity directly relate to domain-specific cognitive impairments in AD spectrum.

Our unbiased MEGI approach identified brain regions that have been implicated to relate to behavior in previous functional and anatomical studies. The dorsolateral prefrontal cortex forms part of a network that is involved in executive performance, attention, working memory, and learning (Dosenbach et al., 2007; Seeley et al., 2007; Vincent et al., 2008; Yeo et al., 2011). Likewise, parietal cortical regions have been linked to visuospatial function (Cabeza and Nyberg, 2000). Consistent with these findings, our results linked connectivity deficits of the left dorsolateral prefrontal cortex to executive dysfunction and connectivity deficits of the left inferior parietal cortex to visuospatial dysfunction. We also found that reduced functional connectivity of left frontal association regions are correlated with episodic memory deficits. This finding is consistent with previous experiments showing that frontal lobe damage impairs both encoding and retrieval of memory (Cabeza and Nyberg, 2000; Goldman-Rakic, 1987, 1988; Greshberg and Shimamura, 1995; Janowsky et al., 1989). It is noteworthy, though, that the medial temporal lobes including the hippocampi, which play an important role in memory, were poorly measured in the present analysis because the current MEGI technology does not allow reliable interrogation of deeper brain structures. Algorithms designed to explore signals from deeper brain structures would resolve this constraint in the future.

We found overlapping brain regions of functional connectivity that correlated with both category and lexical fluency. This observation is contrary to the widely accepted notion that these two tasks are related to different anatomical regions. Previous studies have demonstrated that lexical fluency primarily involves the frontal cortex, whereas category fluency primarily involves the temporal cortex. Some of the most compelling evidence for this distinction comes from investigations of normal aging populations, patients with semantic dementia caused by frontotemporal lobar degeneration, and stroke patients (Baldo et al., 2006; Grogan et al., 2009; Libon et al., 2009). However, other studies have reported that both lexical and category fluency are similarly impaired in patients with frontal lesions (Baldo and Shimamura, 1998; Schwartz and Baldo, 2001). Our results support the hypothesis that patients with frontal lobe pathology have a reduced ability to make strategic and effective searches through memory, independent of whether the search is phonemically or semantically driven (Hirshorn and Thompson-Schill, 2006; Troyer et al., 1998). The mechanism underlying poor category fluency in AD could result from the defective network connectivity of frontal cortices, rather than from an inherent defect of the semantic association regions of the temporal cortex as occurs in semantic dementia.

Future studies are needed to further characterize the disparate networks involved in AD and to address some of the limitations of this study as follows. First, the sample numbers of specific AD-spectrum variants were relatively small. Hence, group contrasts between clinical variants could not be performed. Second, we focused only on the alpha frequency range because there are currently no reliable or reproducible methods to reconstruct source-space functional connectivity in other frequency bands, such as beta or gamma. Third, the patients seen at our specialized center included mostly early-onset disease. Although this approach enabled us to identify specific AD variants, it also limited generalization to the more commonly encountered late-onset AD population. Fourth, while the biomarkers strongly support that our cohort consists of AD pathology, we do not have autopsy confirmation. Future investigations recruiting more numbers, extending to the whole spectrum of AD, with follow-up autopsy confirmations, and with additional analyses of other frequency bands, will further advance our understanding of network dysfunctions in AD spectrum. Additionally, an *a priori* region-of-interest analysis in a new cohort using the regions and correlated tasks that we identified, would be an ideal model for a follow-up study.

In conclusion, the current study details connectivity deficits in AD spectrum by measuring the direct electrical activity of the brain with MEGI. The strength of regional network connectivity is significantly correlated with the performance in specific cognitive domains. MEGI functional connectivity provides a new approach to study dysfunctional networks in AD and other neurodegenerative dementias with high spatial and temporal resolution.

Acknowledgements

We would like to thank Drs. Lennart Mucke, Katherine P. Rankin, and Joel H. Kramer for their valuable feedback on the manuscript; Dr. Gil Rabinovici and Pia Gosh for providing the amyloid imaging; Anna Karydas for her support in genotypic and CSF analysis; Adhimoolam Babu for the support and guidance in VBM analysis; and Naomi Kort for her valuable support in analyzing the MEG data. We also thank all of the study participants and their families for their generous support to our research. This study was supported by the National Institutes of Health grants (K23 AG038357 (K.A.V.), P50 AG023501 and P01 AG19724 (B.L.M.), R21 NS76171 (S.S.N.), R01 DC010145 (S.S.N.), NS066654 (S.S.N.), NS64060 (S.S.N.), National Science Foundation grant BCS-1262297 (S.S.N.)), the John Douglas French Alzheimer's Foundation (K.A.V.), University of California San Francisco Alzheimer's Disease Research Center pilot project grant (K.A.V.), and a gift from the S. D. Bechtel Jr. Foundation.

Appendix A. Supplementary data

Supplementary data associated with this article can be found, in the online version, at http://dx.doi.org/10.1016/j.nicl.2014.07.006.

References

Albert, M.S., DeKosky, S.T., Dickson, D., Dubois, B., Feldman, H.H., Fox, N.C., Gamst, A., Holtzman, D.M., Jagust, W.J., Petersen, R.C., et al., 2011. The diagnosis of mild cognitive impairment due to Alzheimer's disease: Recommendations from the National Institute on Aging-Alzheimer's Association workgroups on diagnostic guidelines for Alzheimer's disease. Alzheimer's & Dementia: the Journal of the Alzheimer's Association 7, 270–279. http://dx.doi.org/10.1016/j.jalz.2011.03.00821514249.

Ashburner, J., Friston, K.J., 1999. Nonlinear spatial normalization using basis functions. Human Brain Mapping 7, 254–26610408769.

Baldo, J.V., Schwartz, S., Wilkins, D., Dronkers, N.F., 2006. Role of frontal versus temporal cortex in verbal fluency as revealed by voxel-based lesion symptom mapping. Journal of the International Neuropsychological Society: JINS 12, 896–900. http://dx.doi.org/10.1017/S135561770606107817064451.

Baldo, J.V., Shimamura, A.P., 1998. Letter and category fluency in patients with frontal lobe lesions. Neuropsychology 12, 259–2679556772.

Benjamini, Y., Hochberg, Y., 1995. Controlling the false discovery rate: A practical and powerful approach to multiple testing. Journal of Royal Statistical Society 57, 289–300.

Brenner, R.P., Ulrich, R.F., Spiker, D.G., Sclabassi, R.J., Reynolds 3rd, C.F., Marin, R.S., Boller, F., 1986. Computerized EEG spectral analysis in elderly normal, demented and depressed subjects. Electroencephalography and Clinical Neurophysiology 64, 483–4922430770.

Buckner, R.L., Snyder, A.Z., Shannon, B.J., LaRossa, G., Sachs, R., Fotenos, A.F., Sheline, Y.I., Klunk, W.E., Mathis, C.A., Morris, J.C., et al., 2005. Molecular, structural, and functional characterization of Alzheimer's disease: Evidence for a relationship between default activity, amyloid, and memory. Journal of Neuroscience: the Official Journal of the Society for Neuroscience 25, 7709–7717. http://dx.doi.org/10.1523/JNEUROSCI.2177-05.200516120771.

Cabeza, R., Nyberg, L., 2000. Imaging cognition II: An empirical review of 275 PET and fMRI studies. Journal of Cognitive Neuroscience 12, 1–4710769304.

Cohen, J., 1992. A power primer. Psychological Bulletin 112, 155–15919565683.

Dalal, S.S., Guggisberg, A.G., Edwards, E., Sekihara, K., Findlay, A.M., Canolty, R.T., Berger, M.S., Knight, R.T., Barbaro, N.M., Kirsch, H.E., et al., 2008. Five-dimensional neuroimaging: Localization of the time-frequency dynamics of cortical activity. NeuroImage 40, 1686–1700. http://dx.doi.org/10.1016/j.neuroimage.2008.01.02318356081.

Dalal, S.S., Zumer, J.M., Guggisberg, A.G., Trumpis, M., Wong, D.D., Sekihara, K., Nagarajan, S. S., 2011. MEG/EEG source reconstruction, statistical evaluation, and visualization with NUTMEG. Computational Intelligence and Neuroscience 2011, 758973. http://dx.doi.org/10.1155/2011/758973214371174.

de Haan, W., Mott, K., van Straaten, E.C., Scheltens, P., Stam, C.J., 2012a. Activity dependent degeneration explains hub vulnerability in Alzheimer's disease. PLoS Computational Biology 8. http://dx.doi.org/10.1371/journal.pcbi.100258222915996.

de Haan, W., Stam, C.J., Jones, B.F., Zuiderwijk, I.M., van Dijk, B.W., Scheltens, P., 2008. Resting-state oscillatory brain dynamics in Alzheimer disease. Journal of Clinical Neurophysiology: Official Publication of the American Electroencephalographic Society 25, 187–193. http://dx.doi.org/10.1097/WNP.0b013e31817da18418677182.

de Haan, W., van der Flier, W.M., Koene, T., Smits, L.L., Scheltens, P., Stam, C.J., 2012b. Disrupted modular brain dynamics reflect cognitive dysfunction in Alzheimer's disease. Neuroimage 59, 3085–3093. http://dx.doi.org/10.1016/j.neuroimage.2011.11.05522154957.

Devanand, D.P., Pradhaban, G., Liu, X., Khandji, A., De Santi, S., Segal, S., Rusinek, H., Pelton, G. H., Honig, L.S., Mayeux, R., et al., 2007. Hippocampal and entorhinal atrophy in mild cognitive impairment: Prediction of Alzheimer disease. Neurology 68, 828–836. http://dx.doi.org/10.1212/01.wnl.0000256697.20968.d717353470.

Dosenbach, N.U., Fair, D.A., Miezin, F.M., Cohen, A.L., Wenger, K.K., Dosenbach, R.A., Fox, M.D., Snyder, A.Z., Vincent, J.L., Raichle, M.E., et al., 2007. Distinct brain networks for adaptive and stable task control in humans. Proceedings of the National Academy of Sciences of the United States of America 104, 11073–11078. http://dx.doi.org/10.1073/pnas.070432010417576922.

Duffy, F.H., Albert, M.S., McAnulty, G., 1984. Brain electrical activity in patients with presenile and senile dementia of the Alzheimer type. Annals of Neurology 16, 439–448. http://dx.doi.org/10.1002/ana.4101604046497353.

Engel, A.K., Gerloff, C., Hilgetag, C.C., Nolte, G., 2013. Intrinsic coupling modes: Multiscale interactions in ongoing brain activity. Neuron 80, 867–886. http://dx.doi.org/10.1016/j.neuron.2013.09.03824267648.

Fox, M.D., Raichle, M.E., 2007. Spontaneous fluctuations in brain activity observed with functional magnetic resonance imaging. Nature Reviews. Neuroscience 8, 700–711. http://dx.doi.org/10.1038/nrn220117704812.

Gelman, A., Hill, J., Yajima, M., 2012. Why we (usually) don't have to worry about multiple comparisons. Journal of Research on Educational Effectiveness 5, 189–211.

Gelman, A., Rubin, D.B., 1992. Inference from iterative simulation using multiple sequences. Statistical Science 457–472.

Goldman-Rakic, P.S., 1987. Circuitry of primate prefrontal cortex and Regulation of Behavior by representational memory. In: Plum, F. (Ed.), Handbook of Physiology, The Nervous System, Higher Functions of the Brain. American Physiological Society, Bethesda, MD, pp. 373–417.

Goldman-Rakic, P.S., 1988. Topography of cognition: Parallel distributed networks in primate association cortex. Annual Review of Neuroscience 11, 137–156. http://dx.doi.org/10.1146/annurev.ne.11.030188.0010333284439.

Gorno-Tempini, M.L., Hillis, A.E., Weintraub, S., Kertesz, A., Mendez, M., Cappa, S.F., Ogar, J. M., Rohrer, J.D., Black, S., Boeve, B.F., et al., 2011. Classification of primary progressive aphasia and its variants. Neurology 76, 1006–1014. http://dx.doi.org/10.1212/WNL.0b013e31821103e621325651.

Gershberg, F.B., Shimamura, A.P., 1995. Impaired use of organizational strategies in free recall following frontal lobe damage. Neuropsychologia 33, 1305–13338552230.

Grogan, A., Green, D.W., Ali, N., Crinion, J.T., Price, C.J., 2009. Structural correlates of semantic and phonemic fluency ability in first and second languages. Cerebral Cortex (New York, N.Y.: 1991) 19, 2690–2698. http://dx.doi.org/10.1093/cercor/bhp02319293396.

Guggisberg, A.G., Honma, S.M., Findlay, A.M., Dalal, S.S., Kirsch, H.E., Berger, M.S., Nagarajan, S.S., 2008. Mapping functional connectivity in patients with brain lesions. Annals of Neurology 63, 193–203. http://dx.doi.org/10.1002/ana.2122417894381.

Hampson, M., Driesen, N.R., Skudlarski, P., Gore, J.C., Constable, R.T., 2006. Brain connectivity related to working memory performance. Journal of Neuroscience: the Official Journal of the Society for Neuroscience 26, 13338–13343. http://dx.doi.org/10.1523/JNEUROSCI.3408-06.200617182784.

Hanslmayr, S., Gross, J., Klimesch, W., Shapiro, K.L., 2011. The role of alpha oscillations in temporal attention. Brain Research Reviews 67, 331–343. http://dx.doi.org/10.1016/j.brainresrev.2011.04.00221592583.

Hindriks, R., Bijma, F., van Dijk, B.W., van der Werf, Y.D., van Someren, E.J., van der Vaart, A. W., 2011. Dynamics underlying spontaneous human alpha oscillations: Adata-driven approach. Neuroimage 57, 440–451. http://dx.doi.org/10.1016/j.neuroimage.2011.04.04321558008.

Hinkley, L.B., Marco, E.J., Findlay, A.M., Honma, S., Jeremy, R.J., Strominger, Z., Bukshpun, P., Wakahiro, M., Brown, W.S., Paul, L.K., et al., 2012. The role of corpus callosum development in functional connectivity and cognitive processing. PloS One 7, e39804. http://dx.doi.org/10.1371/journal.pone.003980422870191.

Hinkley, L.B., Owen, J.P., Fisher, M., Findlay, A.M., Vinogradov, S., Nagarajan, S.S., 2010. Cognitive impairments in schizophrenia as assessed through activation and connectivity measures of magnetoencephalography (MEG) data. Frontiers in Human Neuroscience 3, 73. http://dx.doi.org/10.3389/neuro.09.073.200921160543.

Hinkley, L.B., Vinogradov, S., Guggisberg, A.G., Fisher, M., Findlay, A.M., Nagarajan, S.S., 2011. Clinical symptoms and alpha band resting-state functional connectivity imaging in patients with schizophrenia: Implications for novel approaches to treatment. Biological Psychiatry 70, 1134–1142. http://dx.doi.org/10.1016/j.biopsych.2011.06.02921861988.

Hirshorn, E.A., Thompson-Schill, S.L., 2006. Role of the left inferior frontal gyrus in covert word retrieval: Neural correlates of switching during verbal fluency. Neuropsychologia 44, 2547–2557. http://dx.doi.org/10.1016/j.neuropsychologia.2006.03.03516725162.

Janowsky, J.S., Shimamura, A.P., Kritchevsky, M., Squire, L.R., 1989. Cognitive impairment following frontal lobe damage and its relevance to human amnesia. Behavioral Neuroscience 103, 548–5602736069.

Jelic, V., Shigeta, M., Julin, P., Almkvist, O., Winblad, B., Wahlund, L.O., 1996. Quantitative electroencephalography power and coherence in Alzheimer's disease and mild cognitive impairment. Dementia (Basel, Switzerland) 7, 314–3238915037.

Jeong, J., 2004. EEG dynamics in patients with Alzheimer's disease. Clinical Neurophysiology: Official Journal of the International Federation of Clinical Neurophysiology 115, 1490–1505. http://dx.doi.org/10.1016/j.clinph.2004.01.00115203050.

Klimesch, W., 1999. EEG alpha and theta oscillations reflect cognitive and memory performance: A review and analysis. Brain Research. Brain Research Reviews 29, 169–19510209231.

Kramer, J.H., Jurik, J., Sha, S.J., Rankin, K.P., Rosen, H.J., Johnson, J.K., Miller, B.L., 2003. Distinctive neuropsychological patterns in frontotemporal dementia, semantic dementia, and Alzheimer disease. Cognitive and Behavioral Neurology: Official Journal of the Society for Behavioral and Cognitive Neurology 16, 211–21814665820.

Libon, D.J., McMillan, C., Gunawardena, D., Powers, C., Massimo, L., Khan, A., Morgan, B., Farag, C., Richmond, L., Weinstein, J., et al., 2009. Neurocognitive contributions to verbal fluency deficits in frontotemporal lobar degeneration. Neurology 73, 535–542. http://dx.doi.org/10.1212/WNL.0b013e3181b2a4f519687454.

Martin-Loeches, M., Gil, P., Jimenez, F., Exposito, F.J., Miguel, F., Cacabelos, R., Rubia, F.J., 1991. Topographic maps of brain electrical activity in primary degenerative dementia of the Alzheimer type and multiinfarct dementia. Biological Psychiatry 29, 211–2232015328.

Martino, J., Honma, S.M., Findlay, A.M., Guggisberg, A.G., Owen, J.P., Kirsch, H.E., Berger, M.S., Nagarajan, S.S., 2011. Resting functional connectivity in patients with brain tumors in eloquent areas. Annals of Neurology 69, 521–532. http://dx.doi.org/10.1002/ana.2216721400562.

McKhann, G.M., Knopman, D.S., Chertkow, H., Hyman, B.T., Jack Jr., C.R., Kawas, C.H., Klunk, W.E., Koroshetz, W.J., Manly, J.J., Mayeux, R., et al., 2011. The diagnosis of dementia due to Alzheimer's disease: Recommendations from the National Institute on Aging-Alzheimer's Association workgroups on diagnostic guidelines for Alzheimer's disease. Alzheimer's amp; Dementia: the Journal of the Alzheimer's Association 7, 263–269. http://dx.doi.org/10.1016/j.jalz.2011.03.00521514250.

Mendez, M.F., Ghajarania, M., Perryman, K.M., 2002. Posterior cortical atrophy: Clinical characteristics and differences compared to Alzheimer's disease. Dementia and Geriatric Cognitive Disorders 14, 33–40 58331] [Pubmed: 12053130].

Morris, J.C., 1993. The clinical dementia rating (CDR): Current version and scoring rules. Neurology 43, 2412–24148232972.

Nolte, G., Bai, O., Wheaton, L., Mari, Z., Vorbach, S., Hallett, M., 2004. Identifying true brain interaction from EEG data using the imaginary part of coherency. Clinical Neurophysiology: Official Journal of the International Federation of Clinical Neurophysiology 115, 2292–2307. http://dx.doi.org/10.1016/j.clinph.2004.04.02915351371.

Osipova, D., Ahveninen, J., Jensen, O., Ylikoski, A., Pekkonen, E., 2005. Altered generation of spontaneous oscillations in Alzheimer's disease. Neuroimage 27, 835–841. http://dx.doi.org/10.1016/j.neuroimage.2005.05.01115961323.

Palva, J.M., Monto, S., Kulashekhar, S., Palva, S., 2010. Neuronal synchrony reveals working memory networks and predicts individual memory capacity. Proceedings of the National Academy of Sciences of the United States of America 107, 7580–7585. http://dx.doi.org/10.1073/pnas.091311310720368447.

Plummer, M., Best, N., Cowles, K., Vinesh, K., 2006. CODA: Convergence diagnosis and output analysis for MCMC. R News 6, 7–11.

Possin, K.L., Lamarre, A.K., Wood, K.A., Mungas, D.M., Kramer, J.H., 2014. Ecological validity and neuroanatomical correlates of the NIH EXAMINER Executive composite score. Journal of the International Neuropsychological Society: JINS 20, 20–28. http://dx.doi.org/10.1017/S135561771300061123764015.

Rabinovici, G.D., Furst, A.J., Alkalay, A., Racine, C.A., O'Neil, J.P., Janabi, M., Baker, S.L., Agarwal, N., Bonasera, S.J., Mormino, E.C., et al., 2010. Increased metabolic vulnerability in early-onset Alzheimer's disease is not related to amyloid burden. Brain: A Journal of Neurology 133, 512–528. http://dx.doi.org/10.1093/brain/awp32620080878.

Schwartz, S., Baldo, J., 2001. Distinct patterns of word retrieval in right and left frontal lobe patients: A multidimensional perspective. Neuropsychologia 39, 1209–121711527558.

Seeley, W.W., Crawford, R.K., Zhou, J., Miller, B.L., Greicius, M.D., 2009. Neurodegenerative diseases target large-scale human brain networks. Neuron 62, 42–52. http://dx.doi.org/10.1016/j.neuron.2009.03.02419376066.

Seeley, W.W., Menon, V., Schatzberg, A.F., Keller, J., Glover, G.H., Kenna, H., Reiss, A.L., Greicius, M.D., 2007. Dissociable intrinsic connectivity networks for salience processing and executive control. Journal of Neuroscience: the Official Journal of the Society for Neuroscience 27, 2349–2356. http://dx.doi.org/10.1523/JNEUROSCI.5587-06.200717329432.

Singer, W., 1999. Neuronal synchrony: A versatile code for the definition of relations? Neuron 24, 49–6510677026.

Stam, C.J., de Haan, W., Daffertshofer, A., Jones, B.F., Manshanden, I., van Cappellen van Walsum, A.M., Montez, T., Verbunt, J.P., de Munck, J.C., van Dijk, B.W., et al., 2009. Graph theoretical analysis of magnetoencephalographic functional connectivity in Alzheimer's disease. Brain: A Journal of Neurology 132, 213–224. http://dx.doi.org/10.1093/brain/awn26218952674.

Stam, C.J., Jones, B.F., Manshanden, I., van Cappellen van Walsum, A.M., Montez, T., Verbunt, J.P., de Munck, J.C., van Dijk, B.W., Berendse, H.W., Scheltens, P., 2006. Magnetoencephalographic evaluation of resting-state functional connectivity in Alzheimer's disease. NeuroImage 32, 1335–1344. http://dx.doi.org/10.1016/j.neuroimage.2006.05.03316815039.

Tarapore, P.E., Martino, J., Guggisberg, A.G., Owen, J., Honma, S.M., Findlay, A., Berger, M.S., Kirsch, H.E., Nagarajan, S.S., 2012. Magnetoencephalographic imaging of resting-state functional connectivity predicts postsurgical neurological outcome in brain gliomas. Neurosurgery 71, 1012–1022. http://dx.doi.org/10.1227/NEU.0b013e31826d2b7822895403.

Troyer, A.K., Moscovitch, M., Winocur, G., Alexander, M.P., Stuss, D., 1998. Clustering and switching on verbal fluency: The effects of focal frontal- and temporal-lobe lesions. Neuropsychologia 36, 499–5049705059.

Vincent, J.L., Kahn, I., Snyder, A.Z., Raichle, M.E., Buckner, R.L., 2008. Evidence for a frontoparietal control system revealed by intrinsic functional connectivity. Journal of Neurophysiology 100, 3328–3342. http://dx.doi.org/10.1152/jn.90355.200818799601.

Westlake, K.P., Hinkley, L.B., Bucci, M., Guggisberg, A.G., Byl, N., Findlay, A.M., Henry, R.G., Nagarajan, S.S., 2012. Resting state alpha-band functional connectivity and recovery after stroke. Experimental Neurology 237, 160–169. http://dx.doi.org/10.1016/j.expneurol.2012.06.02022750324.

Yeo, B.T., Krienen, F.M., Sepulcre, J., Sabuncu, M.R., Lashkari, D., Hollinshead, M., Roffman, J.L., Smoller, J.W., Zöllei, L., Polimeni, J.R., et al., 2011. The organization of the human cerebral cortex estimated by intrinsic functional connectivity. Journal of Neurophysiology 106, 1125–1165. http://dx.doi.org/10.1152/jn.00338.201121653723.

Zhou, J., Gennatas, E.D., Kramer, J.H., Miller, B.L., Seeley, W.W., 2012. Predicting regional neurodegeneration from the healthy brain functional connectome. Neuron 73, 1216–1227. http://dx.doi.org/10.1016/j.neuron.2012.03.00422445348.